Macromolecules

ARTICLE

pubs.acs.org/Macromolecules

Bent-Core Based Main-Chain Polymers Showing the Dark Conglomerate Liquid Crystal Phase

Nélida Gimeno,[†,∥] Antoni Sánchez-Ferrer,[‡,∥] Nerea Sebastián,[§] Raffaele Mezzenga,[‡] and M. Blanca Ros[†,*]

[†]Departamento de Química Orgánica, Facultad de Ciencias, Instituto de Ciencia de Materiales de Aragón, Universidad de Zaragoza, CSIC, 50009 Zaragoza, Spain

[‡]Institute of Food, Nutrition & Health, Food & Soft Materials Science Group, ETH Zurich, Schmelzbergstrasse 9, LFO, E23-29, CH-8092 Zürich, Switzerland

[§]Departamento de Física Aplicada II, Facultad de Ciencia y Tecnología, Universidad del País Vasco, Apdo. 644, 48080-Bilbao, Spain

Supporting Information

ABSTRACT: We report the synthesis and characterization of main-chain liquid-crystalline polymers via the hydrosilylation polyaddition of a divinyl terminated bent-core mesogenic monomer and tetramethyldisiloxane. Interestingly, these bent-core main-chain polymers form the "dark conglomerate" mesophase (DC) in broad ranges of temperature. This unique chiral isotropic fluid phase induced from achiral molecules vitrifies keeping at room temperature the chiral domains characteristics of this mesophase. Furthermore, while electric fields switch the bent-core moieties at the molecular level, strong electric fields are able to change the lamellar structure of the DC to a conventional SmCP phase.

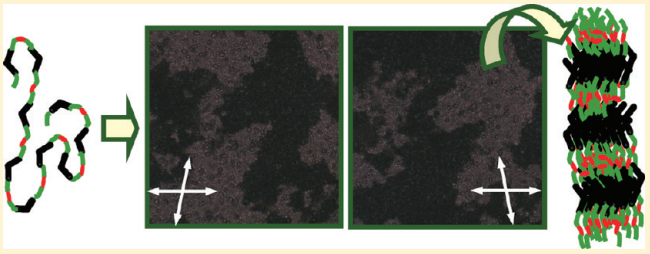

In the past few years, bent-core liquid crystals (BCLC) have become a prime topic of research in the field of liquid crystals due to the singular properties of this type of materials.[1,2] At the beginning, attention was mostly focusing on the structure-properties relationship of this novel kind of soft materials. Modifications in the different parts of the bent-core structure were assayed in order to induce changes, generally on the type of mesophase, the transition temperatures or the phase sequences.[1b−d] Additionally, appealing and diverse responses have been found for bent-core liquid crystals. Specifically, by using these nonchiral molecules, ferro-, antiferro-[2] and piezoelectricity[3] or nonlinear optical activity,[4] optical biaxiality,[5] or flexoelectric behavior[2,6] have been reported for bent-core based mesomorphic materials, realizing their attractive potential as new functional materials.

The singular properties of this kind of liquid-crystalline materials arise from their lamellar [SmCP (polar smectic C mesosphase), SmAP (polar smectic A mesosphase), DC ("dark conglomerate" mesophase), B7, B4, etc][1,7] or columnar mesophases [Col_r, Col_{ob}, etc],[1] different from the classic calamitic or discotic ones. Consequently, the variety of mesophases exhibited by BCLCs has also become a main research focus in the field due to their novelty and peculiarities. Since their discovery, the understanding of both the organization of the molecules within the different phases and the origin of their atypical properties, BCLCs have caught the attention of researchers. All these efforts have resulted in an improved knowledge of the mesophases, but important unsolved issues remain yet to be assessed. Among them, to understand and to control the occurrence of mesophases leading to the chiral resolution of racemic bent-core mesogens into enantiopure domains, proposed to be originated through the presence of chiral conformational states for bent-core molecules at the molecular level[1c] and their singular supramolecular arrangements, such as in the B4 phase[8] or the so-called "dark conglomerate" (DC) phase,[9] are nowadays two main goals within this field of investigation.

One of the most remarkable phenomena in the physics of achiral bent-core liquid crystals is the spontaneous segregation of macroscopic chiral domains in the mesophase (spontaneous *desymmetrization*); an especially important case happens when the mesophase is optically isotropic, and this is the case for the DC phase.

A singularity that distinguishes liquid crystals is they are anisotropic fluids; the DC mesophase is considered an exception. The DC phase is a spontaneous chiral, optically isotropic fluid formed by achiral bent-core liquid crystal molecules, characterized by well-defined locally deformed liquid-crystalline smectic layers. The DC layer system is locally lamellar but globally disordered, with the layer normal ordered only for very short distances, resulting in independently oriented domains whose characteristic dimensions are smaller than the light wavelength. Hough et al.[10] have recently proved that in this DC phase the chiral coupling of local tilt, polarization and layer deformation, limits the orientational and translational order, with handedness

Received: September 16, 2011
Revised: November 5, 2011
Published: November 21, 2011

Scheme 1. Synthetic Route Followed for the Preparation of Polymers P1 and P2

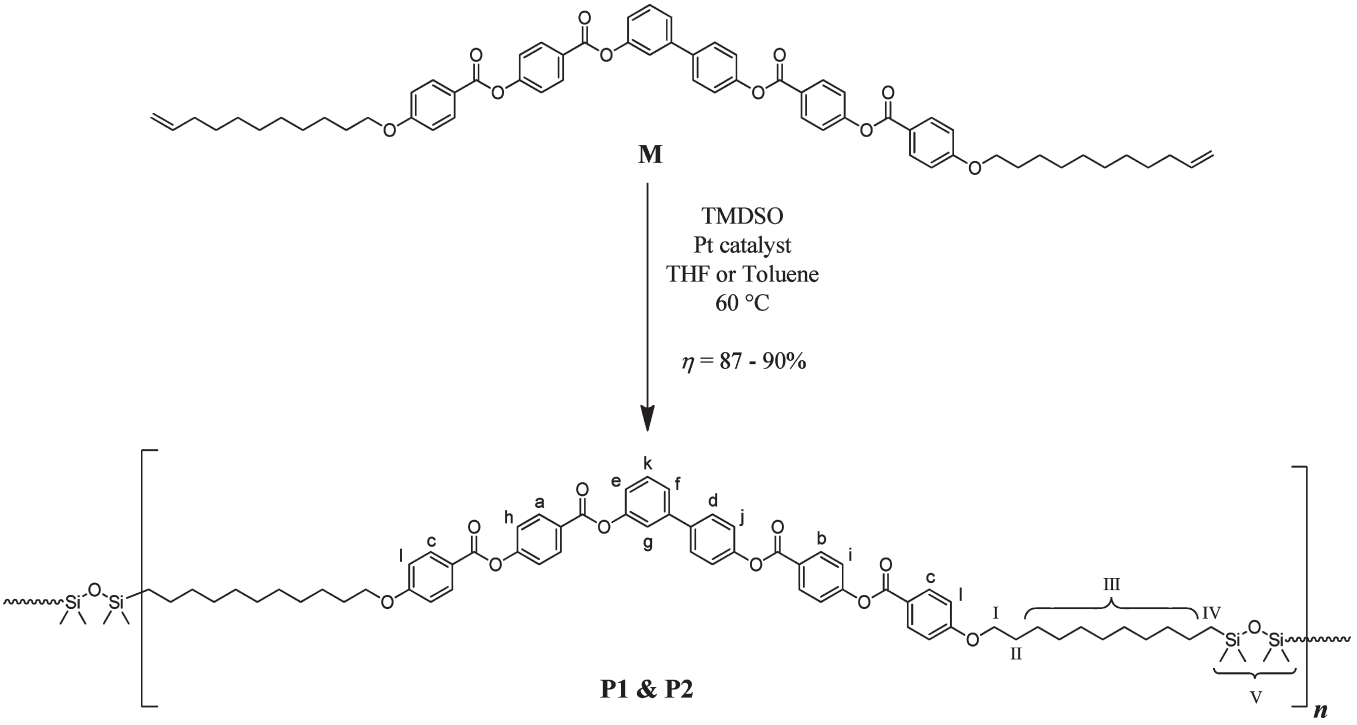

as the only macroscopic ordering. The DC phase has little or no birefringence and thus are nearly dark between crossed polarizers, only at the borderlines between domains sometimes birefringent defects can be observed. However, they provide spontaneous macroscopic chirality very robust, manifested by conglomerate domains up to hundreds of micrometers in size. On the basis of these unique characteristics, interests from basic supramolecular-knowledge to photonic applications possibilities as controlled-dimensional periodic dielectric media are in mind for materials showing this mesophase.

Even though a number of bent-core molecules[10] have been reported to form this optically isotropic phase, it can be said that bent-core silylated materials have revealed a strong ability to promote this type of phase; furthermore the segregation and steric effects caused by the presence of voluminous silicon-substituted units have been proposed as the origin of this trend.[11] Among them, only few examples of silylated polymers showing a DC phase have been reported so far; a side-chain siloxane with a low concentration of bent-core units,[12] or a couple of copolymers containing siloxane units, but the full characterization of the materials have not been achieved due to their high viscosities.[13]

In general, research on bent-core based macromolecules (side-chain or main-chain polymers, networks or dendrimers) is still very limited. However, as it has been made evident for classic liquid crystals, BCLC polymers seem attractive materials as they could combine the unique properties of bent-shaped liquid crystals previously detailed,[2−6] and the great advantages of high molecular weight systems (stability, processability, mechanical properties, flexibility, etc.), most likely around room temperature, either in a mesophase or glassy state.

Former bent-core based macromolecules reported in the literature concern highly cross-linked networks showing SmCP-like order.[14] However, most of the work has been focused on side-chain polymers and both hydrogen bonding[15] and more often covalent approaches, have been explored to this end. Along with the already mentioned siloxane based BCLCs, acrylate- and methacrylate-based BCLCs have also been reported by Tenetti et al.[16] These systems largely form lamellar liquid crystal mesophases (SmCP)[16a] however, as said above, their high viscosity and glass transition temperature seriously limit their electro-optical response. Similar results have also been published for the few bent-core based dendrimers reported so far.[17] Additionally, singular examples of block copolymers bringing together bent-core based and polystyrene blocks have also been prepared.[16b] In this case; lamellar or columnar mesomorphism can be promoted depending on the content of the bent-core based block.

A less explored and unsuccessful research in order to promote bent-core mesophases, has to do with BCLC main-chain polymers. Block copolymers combining bent-shaped and calamitic units have been prepared by alternating diene metathesis polycondensation (ALMET), leading to nematic materials.[18] Both nematic and smectic mesomorphism have been reported by Choi et al.[19] for bent-shaped azomethine-derivated polymers, synthesized by polycondensation of aldehydes and amines. By using the same polymerization approach, they also have reported recently main-chain polymers based on very acute-angle bent-core structures, claiming the formation of smectic C phases and ferroelectric behavior for one of them.[20]

Herein, we report the first examples of BCLC main-chain polymers, which form a chiral optically isotropic liquid phase, the liquid-crystalline DC phase. Hydrosilylation polyaddition has allowed preparing two macromolecules of different size by using solvents of different polarity and boiling point, namely toluene and tetrahydrofuran. For this purpose, a reactive bent-core

monomer was polymerized using 1,1,3,3-tetramethyldisiloxane as chain extender and divinyltetramethyldisiloxane platinum(0) complex as catalyst. Structural characterization of the materials was carried out by ^{1}H NMR, FTIR and GPC. Their thermal and mesomorphic properties were investigated by differential scanning calorimetry (DSC), polarized optical microscopy (POM), small and wide-angle X-ray scattering (SWAXS) and thermogravimetric analysis (TGA). Moreover, studies of their electro-optical and dielectric behavior have been also performed.

EXPERIMENTAL SECTION

The synthetic route followed to obtain bent-core liquid-crystalline polymers is shown in Scheme 1. The monomer (**M**) was prepared according to a synthetic procedure similar to the one reported in the literature[11j] with minor modifications. Further details on the synthesis and full characterization of the monomer **M** are gathered in the Supporting Information and are in agreement with reported previously.[11j]

Polymers **P1** and **P2** were prepared using the hydrosilylation poly-addition reaction. **P1** was prepared using tetrahydrofuran (THF) as solvent, whereas **P2** was synthesized in toluene. The synthetic procedure and complete characterization of both polymers is given below.

Synthesis and Characterization of the Liquid-Crystalline Polymers. In a 5 mL round-bottomed flask, the monomer (M) (217 mg, 0.223 mmol) and 1,1,3,3-tetramethyldisiloxane (TMDSO) (30 mg, 0.223 mmol) were placed, and 2 mL of solvent (tetrahydrofuran or toluene) and 15 μL of 2.1−2.4%-Pt divinyltetramethyldisiloxane platinum(0) complex (Pt(DVTMDSO)) in xylenes were added. The mixture was heated at 60 °C for 2 days. Then the solvent was evaporated and the viscous product was dissolved in dichloromethane. The solution was poured in cold methanol to precipitate the polymer and centrifuged at 3000 rpm at 0 °C during 15 min. This process was repeated three times and, afterward, the solvent was evaporated. The polymer was freeze-dried during 1 day.

P1. ^{1}H NMR (400 MHz, $CDCl_3$): δ = 8.30 (2H, d, H_a, J = 8.6 Hz), 8.29 (2H, d, H_b, J = 8.6 Hz), 8.16 (4H, d, H_c, J = 8.5 Hz), 7.67 (2H, d, H_d, J = 8.4 Hz), 7.51 (2H, d, H_e and H_f, J = 3.9 Hz), 7.46 (1H, s, H_g), 7.38 (2H, d, H_h and H_i, J = 8.6 Hz), 7.32 (2H, d, H_j, J = 8.3), 7.24 (1H, m, H_k), 6.99 (4H, d, H_l, J = 8.8 Hz), 4.05 (4H, t, H_I, J = 6.5 Hz), 1.83 (4H, H_{II}, m, J = 7.0 Hz), 1.70−1.20 (32H, H_{III}, m). 0.51 (4H, t, H_{IV}, J = 7.2 Hz), 0.04 (12H, s, H_V) ppm. M_n = 12200 g·mol^{-1}, DP = 11. FTIR (ATR-diamond): 3074 (st, ArC−H), 2956 (st, SiC-H), 2922 (st, C−H), 2852 (st, OC-H), 1730 (st, ArCC═O), 1603 (st as, ArC−ArC), 1510 (st sy, ArC−ArC), 1251 (st as, ArC−O−AlC; δ sy, Si-CH_3), 1203 (st as, C−O), 1159 (st sy, C−O), 1057 (st sy, ArC−O−AlC; st, Si−O−Si), 843 (γ, Si−CH_3), 760 (st, Si−C) cm^{-1}. GPC (THF, 1 mL·min^{-1}): M_n = 10300 g·mol^{-1}, M_w = 18100 g·mol^{-1}, PDI = 1.76, DP = 9. Yield: 215 mg (87%).

P2. ^{1}H NMR (400 MHz, $CDCl_3$): δ = 8.30 (2H, d, H_a, J = 8.6 Hz), 8.29 (2H, d, H_b, J = 8.6 Hz), 8.16 (4H, d, H_c, J = 8.5 Hz), 7.67 (2H, d, H_d, J = 8.4 Hz), 7.51 (2H, d, H_e and H_f J = 3.9 Hz), 7.46 (1H, s, H_g), 7.38 (2H, d, H_h and H_i, J = 8.6 Hz), 7.32 (2H, d, H_j, J = 8.3), 7.24 (1H, m, H_k), 6.99 (4H, d, H_l, J = 8.8 Hz), 4.05 (4H, t, H_I, J = 6.5 Hz), 1.83 (4H, H_{II}, m, J = 7.0 Hz), 1.70−1.20 (32H, H_{III}, m). 0.51 (4H, t, H_{IV}, J = 7.2 Hz), 0.04 (12H, s, H_V) ppm. M_n = 23200 g·mol^{-1}, DP = 21. FTIR (ATR-diamond): 3074 (st, ArC−H), 2956 (st, SiC−H), 2922 (st, C−H), 2852 (st, OC−H), 1730 (st, ArCC═O), 1603 (st as, ArC−ArC), 1510 (st sy, ArC−ArC), 1252 (st as, ArC−O−AlC; δ sy, Si-CH_3), 1201 (st as, C−O), 1157 (st sy, C−O), 1055 (st sy, ArC−O−AlC; st, Si−O−Si), 840 (γ, Si−CH_3), 760 (st, Si−C) cm^{-1}. GPC (THF, 1 mL·min^{-1}): M_n = 17000 g·mol^{-1}, M_w = 29800 g·mol^{-1}, PDI = 1.75, DP = 15. Yield: 223 mg (90%).

Apparatus and Techniques. ^{1}H NMR experiments were carried out at room temperature on a Bruker Avance Spectrometer operating at 400 MHz, and using $CDCl_3$ as solvents and as the internal standards.

Fourier-transform infrared (FTIR) spectra of solid samples were recorded at room temperature with a Varian 640 FTIR spectrometer and using a MKII Golden Gate single attenuated total reflection (ATR) system.

Gel permeation chromatography (GPC) analyses were performed at 35 °C using a Viscotek TriSEC 302 GPC system equipped with a triple detector array (refractive index, light scattering, and viscosity). Two PSS SDV linear M analytic columns from Polymer Standards Service (pore size 10 μm, 8.0 × 300 mm) using tetrahydrofuran as an eluent at a flow rate of 1 mL·min^{-1} were used. The molecular weight calibration curve was obtained using polystyrene standards.

Microanalyses were performed with a Perkin-Elmer 2400 microanalyser.

Simultaneous small and wide-angle X-ray scattering (SAXS and WAXS, respectively) experiments were performed using a Rigaku MicroMax-002+ microfocused beam (4 kW,45 kV, 0.88 mA) in order to obtain direct information on the SAXS and WAXS reflections. The Cu K_α radiation ($\lambda_{CuK\alpha}$ = 1.5418 Å) was collimated by three pinhole (0.4, 0.3, and 0.8 mm) collimators. The incident beam was normal to the surface of the sample. The scattered X-ray intensity was detected by a Fuji Film BAS-MS 2025 imaging plate system (15.2 × 15.2 cm^2, 50 μm resolution) and a two-dimensional Triton-200 X-ray detector (20 cm diameter, 200 μm resolution). An effective scattering vector range of 0.05 nm^{-1} < q < 25 nm^{-1} was obtained, where q is the scattering wavevector defined as $q = 4\pi(\sin\theta)/\lambda_{CuK\alpha}$, with a scattering angle of 2θ.

Measurements of the transition temperatures were made on a TA Instruments Q-1000 and Q-2000 differential scanning calorimeter. The apparatus were calibrated with indium (156.6 °C, 28.7 J·g^{-1}) and tin (232.1 °C, 60.5 J·g^{-1}). Thermal stability of the polymers was measured on a TA Instruments STD 2960 under a N_2 atmosphere with a heating rate of 10 °C·min.

The textures of the mesophases were studied with an optical microscope Olympus BH2 with crossed polarizers and connected to a Linkam THS60 hot stage. Photomicrographs were taken with a Sony DXC-950P video camera and an Olympus C-5050 and DP-12 cameras.

The dielectric permittivity was measured on Linkam (5 μm thick) cells using an impedance analyzer HP4192A on heating and on cooling rates of 1 °C·min^{-1}. The spontaneous polarization was measured using the triangular wave method on EHC (7 μm thick) cells where the voltage was supplied by an HP33220A arbitrary waveform generator and a Kepco BOP500 M amplifier. The polarization current was recorded using an HP54624A oscilloscope and HP3458A multimeter.

RESULTS AND DISCUSSION

Synthesis of Polymers. The main-chain liquid-crystalline polymers **P1** and **P2** were obtained with high yields by poly-addition reaction of the monomer **M** and a siloxane-based chain extender in two different solvents, THF and toluene. The polymers were characterized by FTIR and NMR spectroscopy, elemental analysis and GPC in order to confirm their chemical composition and the results obtained were in accordance with expectation. FTIR experiments were performed in order to monitor the disappearance of the silane (Si−H) and double bonds (CH═CH_2). Number-average molar mass (M_n) was slightly lower for the polymer prepared in THF with respect to the one prepared in toluene (10300 g·mol^{-1} vs 17000 g·mol^{-1}). However, the polydispersity indexes had practically the same value of PDI = 1.75, lower than the theoretical value for addition polymerization of 2.0 due to the fractioning during the purification process. A degree of polymerization of 9 and 15 repeating units by GPC could be calculated from these data for **P1** and **P2**, respectively, which are consistent with the analysis of the ending groups by ^{1}H NMR (11 and 21 repeating units, respectively). Further details on these measurements are gathered in Table 1.

Table 1. Number Average Molar Mass (M_n), Weight Average Molar Mass (M_w), Polydispersity Index (PDI), and Number of Repeating Units (DP) for the Polymers P1 and P2

polymer	solvent	yield (%)	M_n(GPC) (g·mol^{-1})	M_w(GPC) (g·mol^{-1})	PDI	DP (GPC)	M_n(NMR) (g·mol^{-1})	DP (NMR)
P1	THF	87	10 300	18 100	1.76	9	12 200	11
P2	toluene	90	17 000	29 800	1.75	15	23 200	21

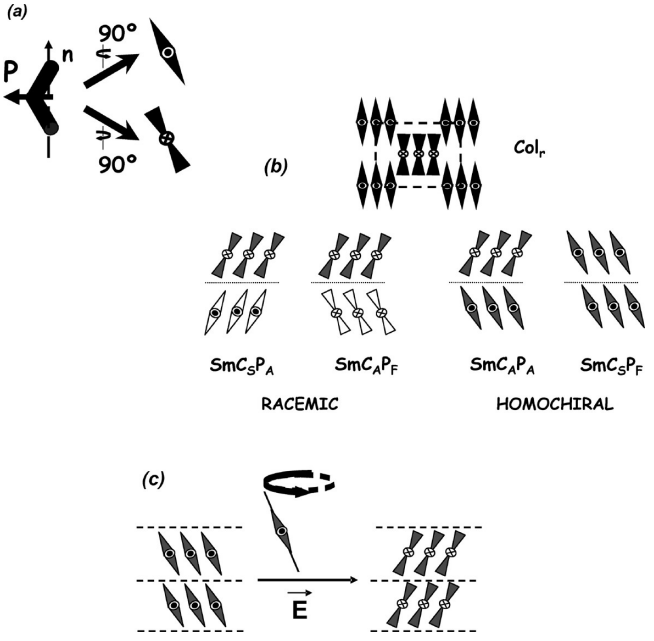

Figure 1. (a) Schematic representations used for tilted bent-shaped molecules: lateral and front views. (b) Bent-core mesophases reported in this study: Col$_r$. (columnar rectangular) and SmCP (polar smectic C) and models proposed for the arrangements of the molecules in the four possible polar tilted smectic C phases (SmCP) and the distorted SmCP (DC)mesphases, which are distinguished by the relative tilt sense and the polar order in the smectic layers. S and A denote synclinic or an anticlinic tilt and F and A refer to a ferro- or antiferroelectricelectric polar order. The color (gray and white) indicates the chirality of the layers, two of them are racemic and two of them homochiral. (c) Ferroelectric molecular switching. It reverses polar direction and tilt direction and retains the layer chirality.

Liquid-Crystalline Properties. All the materials (**M**, **P1**, and **P2**) reported here, were studied by polarizing optical microscopy (POM), differential scanning calorimetry (DSC) and X-ray diffraction (XRD) at variable temperature in order to characterize their liquid-crystalline behavior. Furthermore, the electro-optic responses of the different materials were also investigated by POM under an electric field in order to obtain additional information about the liquid-crystalline phases formed by these molecules and their ability to switch under electric fields.

Mesomorphic behavior of monomer **M** (first heating, crystal 104 °C [35.9 kJ·mol^{-1}]; columnar rectangular 146 °C [18.1 kJ·mol^{-1}]; isotropic liquid; first cooling, isotropic liquid 145 °C [18.9 kJ·mol^{-1}]; columnar rectangular 62 °C [8.3 kJ·mol^{-1}]; crystal) is in agreement with the one previously reported for the same material.[11j] A columnar rectangular (Col$_r$) mesophase with a characteristic mosaic texture was observed under cross polarizer (POM) in a wide range of temperatures on the cooling process (for a graphic representation of the Col$_r$ mesosphase see Figure 1). The nature of the mesophase was confirmed by X-ray diffraction; a columnar rectangular lattice with parameters a = 39.7 Å and b = 49.0 Å were measured (see Figure SI-5, Supporting Information).[11j] Moreover, no switching was observed when applying an electric field to 5 μm Linkam commercial cells filled with the product.

In the case of polymers, the results obtained using the different techniques led us to assign the liquid-crystalline properties gathered in Tables 2 and 3 for the different materials.

DSC thermograms of **P1** and **P2** are shown in Figure 2. As it can be seen, both polymeric materials have a highly liquid-crystalline like nature. Polymer **P1** shows a glass transition (T_g) at 45 °C and the transition to isotropic liquid at 158 °C, whereas the polymer **P2**, prepared in toluene, confirms an increase of both T_g = 54 °C and T_c = 180 °C, which can be ascribed to the high degree of polymerization of this polymer. Concerning the enthalpies changes per repeating unit (in kJ·mol^{-1}) at the clearing points, the calculated values are in good agreement with typical values for bent-core mesophase-to-isotropic liquid transitions in low molecular weight BCLCs.[1c]

Figure 3 shows the TGA curves of both polymers. Decomposition temperature is significantly higher for **P2** versus **P1**, both remaining stable within the mesophase interval. More details are given in Table 2.

Polarized optical microscopy (POM) and X-ray diffraction (XRD) experiments were performed in order to assign the nature of the mesophase of the polymers. Additionally, electro-optical studies were also carried out in order to obtain complementary information concerning the organization of the molecules.

On cooling from the isotropic phase and in the absence of any electric field, mesophase of these polymers appear as fractal nuclei which coalesce to a grainy unspecific texture which appears as very dark (optically isotropic) between crossed polarizers, showing only very small irregularly distributed bright inclusions. The texture is easily noticed if the analyzer is rotated a few degrees (between 5 and 10°) from the crossed position. In these conditions, two domains without birefringence but with opposite optical rotations are clearly detected (Figure 4). The optical activity is clearly visible due to the low birefringence of the DC phase. The color of the domains is interchanged if the direction of rotation of the analyzer is inverted. However, no change is observed when rotating the sample instead of the polarizers, indicating a conglomerate of macroscopically chiral domains with opposite chirality sense and the optically isotropic character of the sample. Likewise it could be observed that the size of the domains depends strongly on the cooling rates. Comparing the first and second rows of Figure 4 it can be observed that for similar cooling rates the size of the domains of compound **P2** is smaller than those of **P1**, which also has less birefringent defects. When shearing the sample between cover and slide at mesophase temperature, the chiral domains disappear and a bright texture is observed (see Supporting Information).

On the basis of these particular features, the formation of a "dark conglomerate" phase (DC) for both polymers is proposed.

Table 2. Thermal Properties of the Polymers P1 and P2, Glass Transition Temperature (T_g), Clearing Temperature (T_c), Isotropization Enthalpy (ΔH_c), Enthalpy per Repeating Unit (ΔH_c/DP), Decomposition Temperature (T_d), and Pyrolisis Residue at T = 600 °C (m_{600}/m_{30})

polymer	DSC scan[a]	T_g (°C)	T_c (°C)	ΔH_c (J·g^{-1})	ΔH_c / DP (kJ·mol^{-1})	T_d (°C)[c]	m_{600}/m_{30} (wt %)[d]
P1	heating	45.5	158.5[b]	18.5	20.4	401	25.8
	cooling	40.0	154.6	14.1	15.5		
P2	heating	54.0	179.6[b]	20.5	22.7	433	18.7
	cooling	55.3	179.2	19.7	21.8		

[a] Data from the second scan at 10 °C·min^{-1}. [b] Maximum of a broad peak. [c] Decomposition temperature given at the onset of the weight loss curve. [d] Pyrolysis residue at 600 °C determined from the weight loss curve.

Table 3. X-ray Diffraction Data of Polymers P1 and P2 at Variable Temperature

polymer	T (°C)	q_1 (nm^{-1})[a]	q_2 (nm^{-1})	q_3 (nm^{-1})	d_{layer} (nm)	ξ_{layer} (nm)	θ (deg)[b]	$d_{mesogen}$ (Å)	$\xi_{mesogen}$ (Å)
P1	70	1.44	2.89	4.26	4.38	60.7	43	4.5	20.3
	140	1.42	2.81	4.19	4.43	66.5	44	4.7	18.2
P2	70	1.45	2.90	4.30	4.33	61.8	42	4.5	21.7
	160	1.44	2.86	4.27	4.36	66.4	43	4.7	15.5

[a] $q_1/q_2/q_3$ = 1:2:3. [b] Length of the mesogen 6.5 nm.

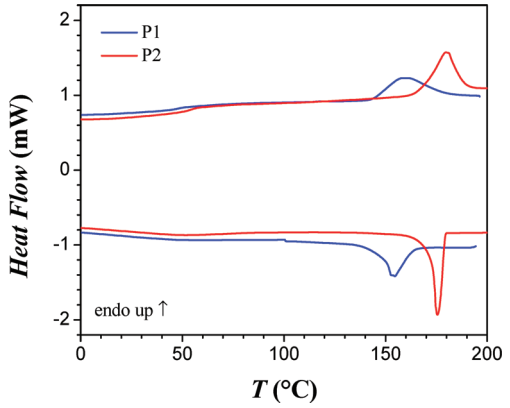

Figure 2. DSC thermograms of polymers **P1** and **P2** at a rate of 10 °C·min^{-1}; corresponding to the heating and cooling processes from the second heating scan.

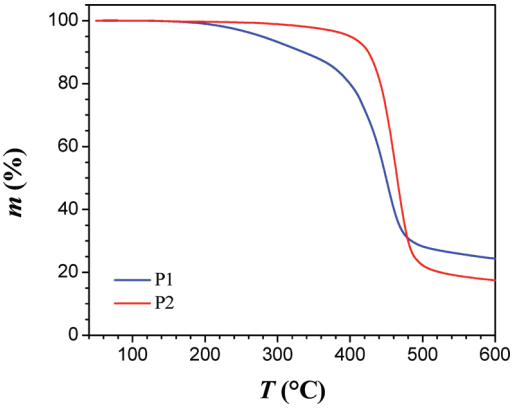

Figure 3. TGA thermograms of polymers **P1** and **P2** at a heating rate of 10 °C·min^{-1}.

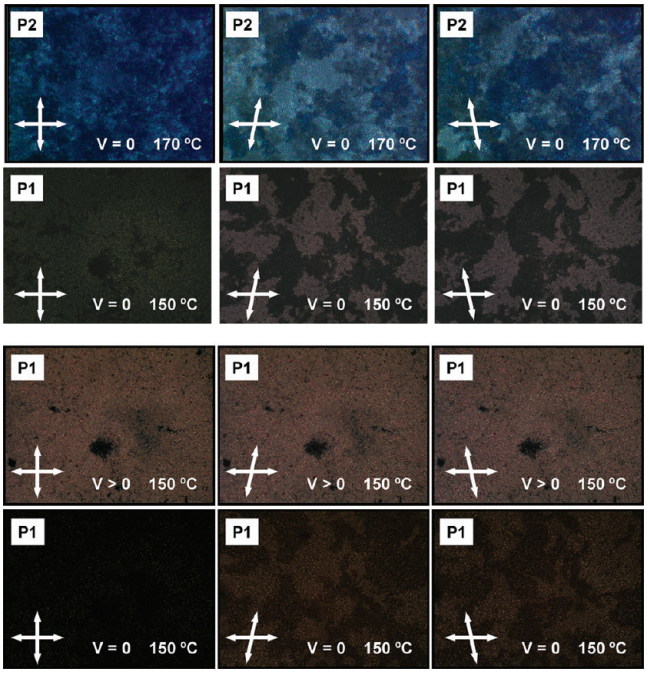

Figure 4. Textures of a thin film of **P2** and **P1** in a 7 μm cells. 1st row: **P2**, at 170 °C (without electric field), under cross polarizers, overcrossing polarizers +θ° and uncrossing polarizers −θ°. Pictures width: 220 μm. 2nd row: **P1**, at 150 °C (without electric field), under cross polarizers, overcrossing polarizers +θ° and uncrossing polarizers −θ°. Pictures width: 1.2 mm. 3rd row: **P1**, at 150 °C (under a triangular-wave electric field (50 Hz, 27 Vpp·μm^{-1}), under cross polarizers, overcrossing polarizers +θ° and uncrossing polarizers −θ°. Pictures width: 1.2 mm. 4th row: **P1**, at 150 °C (after field removal), under cross polarizers, overcrossing polarizers +θ° and uncrossing polarizers −θ°. Pictures width: 1.2 mm.

Different structural models have been reported for DC phase,[9,10] a mesophase characterized by its locally lamellar structure but globally disordered. It has been suggested that the disordered disposition of the domains is not extrinsic but inherent to the nature of the phase itself. According to these models, in this

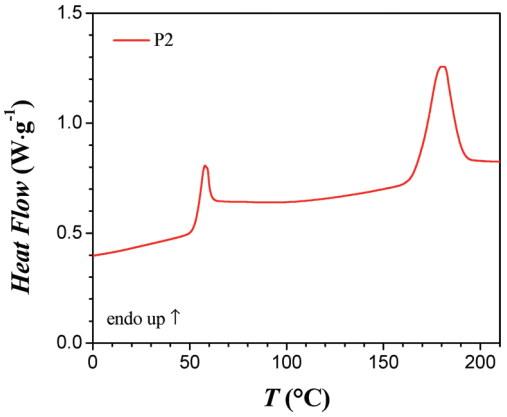

Figure 5. Thermogram of the first heating scan at 20 °C·min^{-1} of a previously thermally treated sample of polymer **P2** several weeks after of this thermal treatment.

phase the smectic planes are strongly folded and the resulting structure is stabilized by a high negative value of the saddle splay elastic constant. The optical isotropy is explained as due to the small size of the flat smectic regions (smaller that the optical wavelength).

When cooling the sample down to room temperature no changes in the texture are observed, the mesosphase order is frozen and the chiral domains can be seen at room temperature for long time. The stability of the mesosphase order has been also checked by DSC experiments, and after several weeks, previously melted samples offer similar transitions; a clear T_g accompanied by a enthalpic relaxation due to the reorganization of the alkyl chains can be observed in the first heating scan of these treated samples (Figure 5). This a typical behavior of polymers with glass transition above room temperature. Thus, interestingly, these main-chain siloxane-based polymers offer the possibility to stabilize DC phases at room temperature, opening new chances for further structural studies and applications of this attractive chiral supramolecular arrangement.

In order to propose the polymer arrangement in the mesophase, X-ray diffraction studies have been performed, and the scattering patterns of the polymers **P1** and **P2** showed three reflections in the low-q region, q_1 = 1.44 nm^{-1}, q_2 = 2.85 nm^{-1}, and q_3 = 4.25 nm^{-1}, corresponding to a layer distance of d_{layer} = 4.4 nm. The ratios q_2/q_1 = 2 and q_3/q_1 = 3 indicate a lamellar distribution of the mesogens. The low intensity of the second reflection q_2 is due to the nearly symmetric volume fraction of both the aromatic ($\phi_{aromatic}$ =0.48) and aliphatic ($\phi_{aliphatic}$ = 0.52) domains. Indeed, for a perfectly symmetric case of $\phi_{aromatic}$ = $\phi_{aliphatic}$, a vanishing second order reflection is expected; in the present case, a slightly asymmetric distribution of the two components and the additional presence of siloxane groups in the polymer backbone, are expected to be responsible for a weak, but still observable second order reflection. Additionally, two broad peaks in the high-q region corresponding to the siloxane interchain (q_s = 10.5 nm^{-1}, d_s = 6.0 Å) distance and mesogen—mesogen distance (q_m = 13.9 nm^{-1}, $d_{mesogen}$ = 4.5 Å) were found. An expansion between the bent-core molecules was found when analyzing the wavevector value at 70 °C - q_m = 13.9 nm^{-1} ($d_{mesogen}$ = 4.5 Å)—and at higher temperatures—q_m = 13.5 nm^{-1} ($d_{mesogen}$ = 4.7 Å). The correlation length of the mesogens $\xi_{mesogen}$ shows the good interaction between the bent-core molecules with values around 20 Å at 70 °C and 15 Å at higher temperatures (Table 3 and Figure 6). These data support the lamellar nature of the liquid-crystalline phase, as the textures pointed out. In accordance to the packing Tschierske's proposals for siloxane-containing bent-core molecules,[11b] the absence of microphase separated siloxane domains might be due to the low silicone content in the flexible domains of the molecule (see Supporting Information, Figure SI-4). From the reflections in the small angle region, the layer spacing d_{layer} could be determined. Thus, layer spacing of 4.43 and 4.36 nm were measured for polymers **P1** and **P2** at temperatures (140 and 150 °C respectively), with respect to the distance between layers of 4.38 nm (**P1**) and 4.33 nm (**P2**) measured at 70 °C. The correlation length ξ_{layer} is in the range of 60−65 nm length scale, which supports the good layering formation at this volume fraction of the two components of the repeating unit in the polymer backbone. Moreover, when experiments were performed at room temperature after heating and cooling processes, diffractograms similar to those obtained at high temperature were also acquired. The diffuse wide angle scattering was maintained at room temperature that confirms the glassy nature of the materials and allows ruling out crystallization processes, as also seen by DSC and POM. When comparing experimental values of the layer spacing with the molecular length of the repeating unit in the extended conformation of the terminal chains, it was possible to calculate tilting angles of the mesogenic units around 43°, accordingly to values reported for bent-core compounds in many tilted mesophases.[2]

All these data validate the lamellar nature of the mesophase promoted by these main-chain polymers, in agreement with the typical X-ray diffraction patterns reported for the DC mesophase, as a variety of SmCP arrangements (for a graphic representation of the SmCP mesosphase see Figure 1). Furthermore, as can be seen from these data, the incorporation of the bent-core structure as part of a polymer chain, allows a significant stabilization of the mesophase as well as a change from columnar to a lamellar organization.

Among the different types of SmCP-like order, the presence of chiral domains can be only explained by an anticlinic and antiferroelectric (SmC_AP_A) or a synclinic and ferroelectric (SmC_SP_F) arrangement of the molecules, since the other two possibilities (SmC_SP_A and SmC_AP_F) are racemic and therefore optically inactive (for a graphic representation of these SmCP mesophases see Figure 1).[1] It has been proposed[1] that a correlation exists between the molecular structure inducing the DC phase and the stabilization of the ferroelectric arrangement or destabilization of the antiferroelectric organization. However, results also confirm that the formation of DC textures is independent of polar order, and layer distortion is also found in nonpolar $SmCP_A$ phases, pointing out that steric and chirality effects are also required.[11e]

In the case of compounds **P1** and **P2**, the DC phase is observed on cooling from the isotropic phase in the absence of an external electric field. However, when cooling under a strong square wave (12 V·μm^{-1} at 10 Hz) a grainy birefringent texture is obtained.[11i,21] The same texture is observed by applying high electric fields to the DC phase (Figure 4). Nonetheless, by any event, the typical birefringent texture with circular domains is not observed in these materials.

In the aim to state the polar nature of the lamellar mesophase promoted by these main-chain polymers **P1** and **P2,** polarization studies have been carried out under different field conditions, for a triangular wave of 50 Hz and 26 V_{pp}·μm^{-1} (Figure 7a), and for a

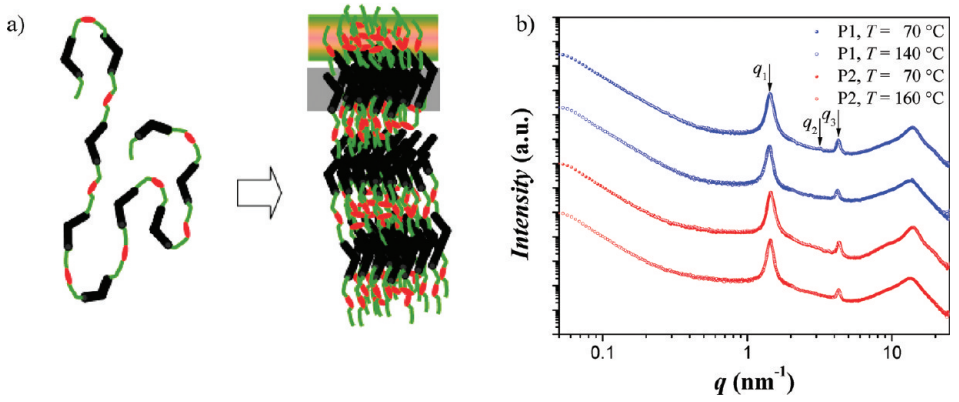

Figure 6. (a) Model of the polymer organization: (rigth) lateral view of the molecular packing in the tilted lamellar mesophase (see also Figure 1a) and (b) X-ray scattering radial distribution in the DC phase for the polymer **P1** (at 70 and 140 °C) and polymer **P2** (at 70 and 160 °C).

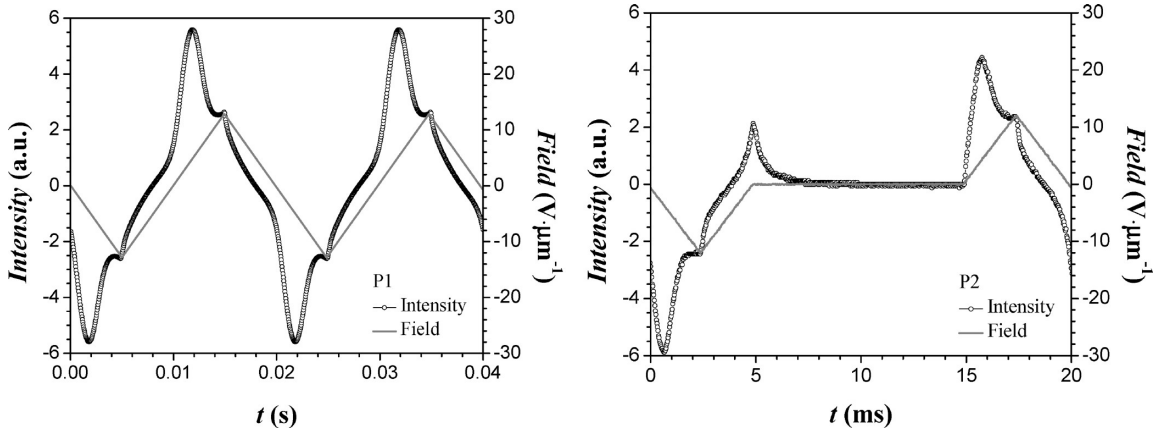

Figure 7. Polarization switching current in the SmCP phase of **P1** (at 150 °C) under a triangular-wave electric field (50 Hz, 26 Vpp·μm^{-1}) and **P2** (at 170 °C) under a modified triangular-wave electric field (50 Hz, 26 Vpp·μm^{-1}).

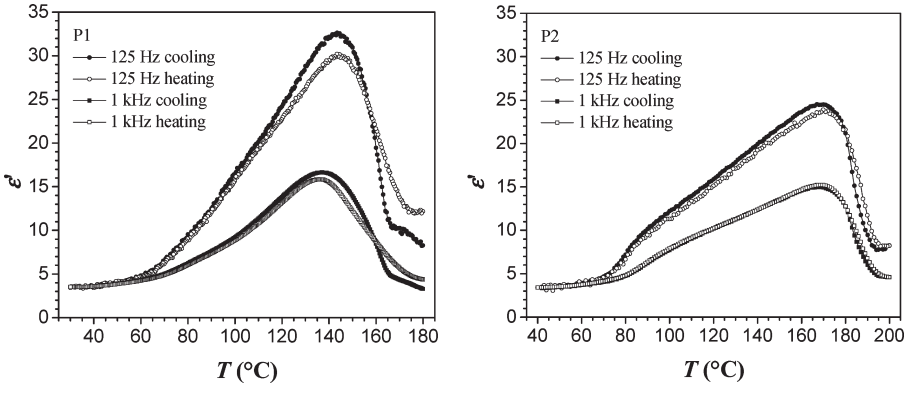

Figure 8. Dielectric permittivity versus temperature for polymers **P1** and **P2**, on heating and cooling runs.

modified triangular wave that includes a plateau at 0 voltage (Figure 7b). As the behavior of both compounds has been found to be similar, Figure 7 shows as an example the switching current for **P1** under a triangular wave and for **P2** under a modified triangular wave. It can be seen that the switching of the field-induced state is ferroelectric-like (Figure 1c), with only one broad peak per half cycle, delayed with respect to the field sign change, as it has been reported for other DC phases of BCLC.[11e,j,l,21] This peak only emerges after the application of a threshold field of 20 $V_{pp}\cdot\mu m^{-1}$ but by reducing the field gradually, the peak is also observed for lower voltages. Macroscopic polarization values of around 500 nC·cm^{-2} for **P1** and 250 nC·cm^{-2} for **P2** in polydomain samples have been obtained.

Concerning the dielectric studies, Figure 8 shows the temperature dependence of the dielectric permittivity for 125 Hz and 1 kHz for both polymers. The results are reproducible in the heating and cooling processes and the dielectric permittivity

dx.doi.org/10.1021/ma202109z |*Macromolecules* 2011, 44, 9586–9594

reaches a value of ca. 30 in the mesophase. These values are frequently found in SmCP mesophases.[2]

We conclude by mentioning that the effect of electric fields on the distorted layer structure depends heavily on the previously applied electric fields. After the removal of square or triangular waves in some occasions the dark texture has been recovered even with fewer defects than before the application of the field, see Figure 4, 4th row, for example.

CONCLUSIONS

Hydrosilylation polyaddition of a bent-core monomer has allowed preparing for the first time bent-core based main-chain liquid-crystalline polymers that form the peculiar "dark conglomerate" mesosphase (DC) in broad ranges of temperature. Interestingly, in the case of the present main-chain siloxane-based polymer, this unique fluid from achiral molecules with segregated homoquiral domains, vitrifies which allows keeping the chiral order at room temperature. Moreover, due to the macromolecular nature of these materials, strong electric fields are needed to affect the locally but globally disordered lamellar structure precluding the evolution to a conventional SmCP phase. These results open new possibilities in the route to the knowledge of this chiral organization but also for the application of this phase as a new source of optical activity in supramolecular systems and for new stimuli-responsive functional materials with useful properties.

ASSOCIATED CONTENT

Supporting Information. Experimental section: Synthesis of monomer **M** and polymers **P1** and **P2** and a summary of ^{1}H NMR and FTIR spectra of monomer and polymers and GPC data of polymers; SAXS and WAXS data of polymers, MOP textures, and DSC and X-ray data of monomer **M**; polarization switching current curves of polymers. This material is available free of charge via the Internet at http://pubs.acs.org.

AUTHOR INFORMATION

Corresponding Author

*Telephone: +34 976 762277. Fax: + 34 976 761209. E-mail: bros@unizar.es.

Author Contributions

‖The first two authors contributed equally to this study.

ACKNOWLEDGMENT

The authors thank the financial support from the Spanish Government (MICINN-FEDER projects MAT2009-14636-C03, Aragon (Project E04) and Basque (Project GI/IT-449-10) governments, and Juan de la Cierva-MICINN and JAE-DOC-CSIC (N.G.) and Universidad del País Vasco (N.S.) fellowship programs are greatly appreciated.

REFERENCES

(1) (a) Reddy, R. A.; Tschierske, C. *J. Mater. Chem.* **2006**, *16*, 907. (b) Wesissflog, W.; Sheenivasa Murthy, H. N.; Diele, S.; Pelzl, G. *Philos. Trans. R. Soc.* **2006**, *364*, 2657. (c) Takezoe, H.; Takanishi, Y. *Jpn. J. Appl. Phys.* **2006**, *45*, 597. (d) Pelzl, G.; Weissflog, W. *Thermotropic Liquid Crystals. Recent Advances*; Ramamoorthy, A., Ed.; Springer: Dordrecht, The Netherlands, 2007, Chapter 1, p 1.

(2) (a) Jákli, A.; Bailey, C.; Harden, J. *Thermotropic Liquid Crystals. Recent Advances*; Ramamoorthy, A., Ed.; Springer: Dordrecht, The Netherlands, 2007, Chapter 2, p 59. (b) Etxebarria, J.; Ros, M. B. *J. Mater. Chem.* **2008**, *18*, 2919.

(3) Jákli, A.; Pintre, I. C.; Serrano, J. L.; Ros, M. B.; de la Fuente, M. R. *Adv. Mater.* **2009**, *21*, 3784.

(4) Pintre, I. C.; Serrano, J. L.; Ros, M. B.; Martínez-Perdiguero, J.; Alonso, I.; Ortega, J.; Folcia, C. L.; Etxebarria, J.; Alicante, R.; Villacampa, B. *J. Mater. Chem.* **2010**, *20*, 2965.

(5) Tschierske, C.; Photinos, D. J. *J. Mater. Chem.* **2010**, *20*, 4263.

(6) (a) Van Le, K.; Araoka, F.; Fodor-Csorba, K.; Ishikawa, K.; Takezoe, H. *Liq. Cryst.* **2009**, *36*, 1119. (b) Harden, J.; Chambers, M.; Verduzco, R.; Luchette, P.; Gleeson, J. T.; Sprunt, S.; Jákli, A. *App. Phys. Lett.* **2010**, *96*, 102907.

(7) Walba, D. *Top. Stereochem.* **2003**, *24*, 457.

(8) (a) Walba, D. M.; Eshdat, L.; Korblova, E.; Shoemaker, R. K. *Cryst. Growth Des.* **2005**, *5*, 2091. (b) Takezoe, H.; Takanishi, Y. *Jpn. J. Appl. Phys.* **2006**, *45*, 597. (c) Reddy, R. A.; Tschierske, C. *J. Mater. Chem.* **2006**, *16*, 907. (d) Hough, L. E.; Jung, H. T.; Krüerke, D.; Heberling, M. S.; Nakata, M.; Jones, C. D.; Chen, D.; Link, D. R.; Zasadzinski, J.; Heppke, G.; Rabe, J. P.; Stocker, W.; Körblova, E.; Walba, D. M.; Glaser, M. A.; Clark, N. A. *Science* **2009**, *325*, 456. (e) Martínez-Perdiguero, J.; Alonso, I.; Folcia, C. L.; Etxebarria, J.; Ortega, J. *J. Mater. Chem.* **2009**, *19*, 5161.

(9) (a) Dantlgraber, G.; Eremin, A.; Diele, S.; Hauser, A.; Kresse, H.; Pelzl, G.; Tschierske, C. *Angew. Chem., Int. Ed.* **2002**, *41*, 2408. (b) Etxebarria, J.; Folcia, C. L.; Ortega, J.; Ros, B. *Phys. Rev. E* **2003**, *67*, 042702. (c) Eremin, A.; Diele, S.; Pelzl, G.; Weissflog, W. *Phys. Rev. Lett.* **2003**, *67*, 020702. (d) Weissflog, W.; Schroder, M. W.; Diele, S.; Pelzl, G. *Adv. Mater.* **2003**, *15*, 630. (e) Liao, G.; Stojadinovic, S.; Pelzl, G.; Weissflog, W.; Sprunt, S.; Jakli, A. *Phys. Rev. E* **2005**, *72*, 021710. (f) Lagerwall, J. P. F.; Giesselmann, F. *ChemPhysChem* **2010**, *11*, 975.

(10) (a) Chen, D.; Shen, Y.; Zhu, C.; Hough, L. E.; Gimeno, N.; Glaser, M. A.; Maclennan, J. E.; Ros, M. B.; Clark, N. A. *Soft Matter* **2011**, *7*, 1879. (b) Hough, L. E.; Spannuth, M.; Nakata, M.; Coleman, D. A.; Jones, C. D.; Dantlgraber, G.; Tschierske, C.; Watanabe, J.; Körblova, E.; Walba, D. M.; Maclennan, J. E.; Glaser, M. A.; Clark, N. A. *Science* **2009**, *325*, 452.

(11) (a) Dantlgraber, G.; Baumeister, U.; Diele, S.; Kresse, H.; Luhmann, B.; Lang, H.; Tschierske, C. *J. Am. Chem. Soc.* **2002**, *124*, 14852. (b) Dantlgraber, G.; Diele, S.; Tschierske, C. *Chem. Commun.* **2002**, 2768. (c) Keith, C.; Reddy, R. A.; Hang, H.; Lang, H.; Tschierske, C. *Chem. Commun.* **2004**, 1898. (d) Kosata, B.; Tamba, G. M.; Baumeister, U.; Pelz, K.; Diele, S.; Pelzl, G.; Galli, G.; Samaritani, S.; Agina, E. V.; Boiko, N. I.; Shibaev, V. P.; Weissflog, W. *Chem. Mater.* **2006**, *18*, 691. (e) Keith, C.; Reddy, R. A.; Hauser, A.; Baumeister, U.; Tschierske, C. *J. Am. Chem. Soc.* **2006**, *128*, 3051. (f) Hahn, H.; Keith, C.; Lang, H.; Reddy, R. A.; Tschierske, C. *Adv. Mater.* **2006**, *18*, 2629. (g) Achten, R.; Koudijs, A.; Giesbers, M.; Marcelis, A. T. M.; Sudhölter, E. J. R.; Schroeder, M. W.; Weissflog, W. *Liq. Cryst.* **2007**, *34*, 59. (h) Reddy, R. A.; Baumeister, U.; Keith, C.; Tschierske, C. *J. Mater. Chem.* **2007**, *17*, 62. (i) Keith, C.; Dantlgraber, G.; Reddy, R. A.; Baumeister, U.; Prehm, M.; Hahn, H.; Lang, H.; Tschierske, C. *J. Mater. Chem.* **2007**, *17*, 3796. (j) Keith, C.; Reddy, R. A.; Prehm, M.; Baumeister, U.; Kresse, H.; Chao, J. L.; Hahn, H.; Lang, H.; Tschierske, C. *Chem.—Eur. J.* **2007**, *13*, 2556. (k) Pan, Q. W.; Chen, X. F.; Fan, X. G.; Shen, Z. H.; Zhou, Q. F. *J. Mater. Chem.* **2008**, *18*, 3481. (l) Zhang, Y.; Baumeister, U.; Tschierske, C.; O'Callaghan, M. J.; Walker, C. *Chem. Mater.* **2010**, *22*, 2869.

(12) Keith, C.; Reddy, R. A.; Tschierske., C. *Chem. Commun.* **2005**, 871.

(13) (a) Achten, R.; Koudijs, A.; Giesbers, M.; Reddy, R. A.; Verhulst, T.; Tschierske, C.; Marcelis, A.; Sudhölter, E. *Liq. Cryst.* **2006**, *33*, 681. (b) Bubnov, A.; Novotná, V.; Pociecha, D.; Kaspar, M.; Hamplova, V.; Galli, G.; Glogarova, M. *Macromol. Chem. Phys.* **2011**, *212*, 191.

(14) (a) Keum, C. D.; Kanazawa, A.; Ikeda, T. *Adv. Mater.* **2001**, *13*, 321. (b) Sentman, A. C.; Gin, D. L. *Angew. Chem., Int. Ed.* **2003**, *42*, 1815. (c) Barbera, J.; Gimeno, N.; Monreal, L.; Pinol, R.; Ros, M. B.; Serrano, J. L. *J. Am. Chem. Soc.* **2004**, *126*, 7190.

(15) (a) Barbera, J.; Gimeno, N.; Pintre, I.; Ros, M B.; Serrano, J. L. *Chem. Commun.* **2006**, *11*, 1212. (b) Wang, L.-Y.; Chiang, I.-H.; Yang, P.-J.; Li, W.-S.; Chao, I.-T.; Lin, H.-C. *J. Phys. Chem. B* **2009**, *113*, 14648. (c) Wang, L.-Y.; Tsai, H.-Y.; Lin, H.-C. *Macromolecules* **2010**, *43*, 1277. (d) Yang, P.; Wang, L.-Y.; Tang, C.; Lin, H.-C. *J. Polym. Sci., Part A: Polym. Chem.* **2010**, *48*, 764.

(16) (a) Chen, X.; Tenneti, K. K.; Li, C. Y.; Bai, Y.; Wan, X.; Fan, X.; Zhou, Q.-F.; Rong, L.; Hsiao, B. S. *Macromolecules* **2007**, *40*, 840. (b) Tenneti, K. K.; Chen, X.; Li, C. Y.; Shen, Z.; Wan, X.; Fan, X.; Zhou, Q. F.; Rong, L.; Hsiao, B. S. *Macromolecules* **2009**, *42*, 3510.

(17) Kardas, D.; Prehm, M.; Baumeister, U.; Pociecha, D.; Reddy, R. A.; Mehl, G. H.; Tschierske, C. *J. Mater. Chem.* **2005**, *15*, 1722.

(18) Demel, S.; Slugovc, C. F. S.; Fodor-Csorba, K.; Galli, G. *Macromol. Rapid Commun.* **2003**, *24*, 636.

(19) Choi, E. J.; Ahn, J. C.; Chien, L. C.; Lec, C. K.; Zin, W. C.; Kim, D. C.; Shin, S. T. *Macromolecules* **2004**, *37*, 71.

(20) Choi, E. J.; Kim, E. C.; Ohk, C. W.; Zin, W. C.; Lee, J. H.; Lim, T. K. *Macromolecules* **2010**, *43*, 2865.

(21) Gimeno, N.; Barbera, J.; Serrano, J. L.; Ros, M. B.; de la Fuente, M. R.; Alonso, I.; Folcia, C. L. *Chem. Mater.* **2009**, *21*, 4620.